Atmospheric Pollution Research 12 (2021) 65–74

Contents lists available at ScienceDirect

Atmospheric Pollution Research

journal homepage: www.elsevier.com/locate/apr

Performance of MODIS C6.1 Dark Target and Deep Blue aerosol products in Delhi National Capital Region, India: Application for aerosol studies

Vipasha Sharma [a], Swagata Ghosh [a,*], Muhammad Bilal [b], Sagnik Dey [c], Sultan Singh [d]

[a] Amity Institute of Geoinformatics and Remote Sensing (AIGIRS), Amity University, Sector 125, Noida, U.P., 201313, India
[b] Lab of Environmental Remote Sensing (LERS), School of Marine Science, Nanjing University of Information Science and Technology, Nanjing, 210044, China
[c] Centre for Atmospheric Sciences, Indian Institute of Technology Delhi, Hauz Khas, New Delhi, 110016, India
[d] Haryana Space Applications Centre Node, Gurgaon New labour court building, Mini Secretariat, Sector 11, Gurugram, Haryana, 122001, India

A R T I C L E I N F O

Keywords:
AOD
MODIS C6.1
AERONET
DB
DT
NCR

A B S T R A C T

Delhi National Capital Region (NCR) of India is one of the most polluted regions in the world, yet only two ground-based monitoring sites under the AERosol RObotic NETwork (AERONET) measuring Aerosol Optical Depth (AOD) are operational in this region. Here, we assessed the performance of Terra and Aqua MODIS collection 6.1 AOD product to understand their applicability for studying seasonal and spatial variations of AOD over Delhi-NCR. We compared Deep Blue AOD at 550 nm retrieved at 10 km resolution (DB_{10K}), and Dark Target AOD retrieved at 3 km (DT_{3K}) and 10 km (DT_{10K}) resolutions against AOD from these two AERONET sites (Gual Pahari and Amity University) during 2010–2019 keeping in mind the uncertainty range represented as expected error (EE) envelope [$EE = \pm (0.03 + 20\% \ AOD_{AERONET})$ for DB_{10K}, $EE = \pm (0.05 + 20\% \ AOD_{AERONET})$ and $EE = \pm (0.05 + 15\% \ AOD_{AERONET})$ for DT_{3K} and DT_{10K} respectively]. Our evaluation reveals the following statistics: correlation coefficients (R) of 0.44, 0.74, and 0.77 for DB_{10K}, $DT_{3K,}$ and DT_{10K} AODs from TERRA and 0.7, 0.79, and 0.72 from AQUA, respectively and root mean square errors of 0.26, 0.01, and 0.17 for AODs from TERRA and 0.24, 0.20, and 0.24 for AODs from AQUA, respectively. Our results demonstrate better reliability of the DT AOD products relative to DB over urbanized areas in North India. Emission from industries, power plants, brick kilns, enhances aerosol loading after a light precipitation event.

1. Introduction

Aerosols alter the weather and climate through direct and indirect effects (Boucher and Haywood, 2001; Kaufman et al., 2002). The foremost requirement to minimize aerosol forcing's uncertainty is spatially and temporally continuous data of aerosol properties, such as aerosol optical depth (AOD), aerosol size distribution, and their ability to scatter and absorb radiation. In the early part of the last decade of the 20th century, a network known as Aerosol Robotic Network (AERONET) was developed by NASA to systematically measure columnar aerosol optical properties using a sunphotometer (Holben et al., 1998). Parallel efforts led to the development of Skynet (Campanelli et al., 2015; Sano et al., 2003) and the multi-wavelength radiometer network of the Indian Space Research Organization (Kompalli et al., 2010; Moorthy et al., 1989). Though these networks gradually expanded over the years, covering diverse geographical regions, a substantial spatial gap still exists, especially in developing countries.

Satellite remote sensing evolved to complement the surface-based measurements of aerosol characteristics and fill the spatial gap. In the 20th century, passive sensors were only capable of measuring aerosols over the oceans. Long-term data from Global Aerosol Climatology Project (Mishchenko et al., 2007) revealed a declining trend in global AOD during 1991–2005, in agreement with an increasing trend in surface solar irradiance (Wild et al., 2005). The aerosol monitoring from space experienced a paradigm shift (Kaufman et al., 2002) with the launch of NASA's Earth-observing satellite Terra that carried two sensors -Moderate Resolution Imaging Spectroradiometer, MODIS (Sai Suman et al., 2014) and Multiangle Imaging Spectroradiometer, MISR (Mukherjee and Vinoj, 2020), and Aqua that carried MODIS capable of retrieving aerosol properties over land and ocean. These sensors continue to provide aerosol data over 20+ years that helped (i) understanding the global patterns of AOD and their temporal trends (Alpert

Peer review under responsibility of Turkish National Committee for Air Pollution Research and Control.
* Corresponding author.
E-mail addresses: swagata.gis@gmail.com, sghosh1@amity.edu (S. Ghosh).

https://doi.org/10.1016/j.apr.2021.01.023
Received 28 September 2020; Received in revised form 25 January 2021; Accepted 25 January 2021
Available online 30 January 2021

et al., 2012; Tong et al., 2020); (ii) reducing the uncertainty in aerosol radiative forcing (Kahn, 2012); (iii) improving our understanding of the aerosol-cloud interaction (Bender et al., 2019) and (iv) examining the environmental impacts of aerosols (Colbeck and Lazaridis, 2010; Ren-Jian et al., 2012).

The aerosol retrieval algorithms of MODIS and MISR have been updated several times during the mission to improve upon the limitations of the previous versions of the algorithm. For example, MODIS aerosol product has changed from the collection, C4 to C6.1 (with intermediate versions C5, C5.1, and C6 in between). In addition to the global validation routinely carried out by the MODIS science team (e.g., Christopher and Gupta, 2020), regional validation is also important to understand such products' utility for local applications (Bilal et al., 2019; Huang et al., 2019; Tian et al., 2018; Tuna Tuygun et al., 2020). Satellite aerosol products have been proven to be highly useful in aerosol studies over the Indian subcontinent (Dey and Di Girolamo, 2010; Mangla and Chakra, 2020; Mhawish et al., 2017; Tripathi et al., 2005) where ground-based observations are scanty.

The majority of the previous satellite-based aerosol studies in India analyzed the older versions of the aerosol products; only a handful of studies validated C6.1 aerosol products (Mangla et al., 2020; Mhawish et al., 2017; Sayer et al., 2013). Most importantly, none of the previous studies focused on the Delhi National Capital Region (NCR) except one study (Srivastava et al., 2014) that used the older MODIS C5 aerosol product. Delhi NCR has been identified as one of the most polluted metropolitan areas globally (WHO, 2016). However, in such a dynamic, highly urbanized, and polluted region, only two AERONET sites are available (Fig. 1), which reinforces the need to apply satellite-based aerosol products for a range of applications, including the use of AOD for estimating surface fine particulate matter, $PM_{2.5}$ (Dey et al., 2012; Chowdhury et al., 2019). Therefore, the present study aims to carry out a rigorous evaluation of MODIS AOD C6.1 products with AERONET observations within Delhi NCR for ten years (2010–2019) and apply it to understand the spatio-temporal variations of the aerosol properties in the region.

2. Study area, data, and methodology

2.1. Study area

Delhi NCR covers the entire National Capital Territory (NCT) of Delhi and 13, 8, and 2 districts of the adjacent states of Haryana, Uttar Pradesh, and Rajasthan, respectively, with a total area of 53,600 km^2 (Jalan, 2019). It is a region of mixed urban and rural land covers with an urbanization level of 62.6% and a population of 46 million (Census of India, 2011). In the present study, four Delhi NCR districts (Gurugram, Ghaziabad, Faridabad, and Gautam Buddha Nagar) are chosen (Fig. 1). These four districts share similar climatic characteristics with four distinct seasons – pre-monsoon/summer (March–May), monsoon (June–September), post-monsoon (October–November), and winter (December–February). The average temperature varies from 25 °C to 49 °C during summer and from 22 °C to 2 °C during winter. Dust storms from Rajasthan and snowfall near Kumaon and Garhwal affect the weather significantly of the study area.

Gurugram (28.45° N, 77.02° E) ranks as the 6th most polluted city in the South Asian region (*2018* World Air Quality Report, 2018; Dahiya et al., 2017). It is one of the leading financial and commercial hubs with the highest Human Development Index of 0.88 in India (SDG Vision Haryana, 2030, 2017). Ghaziabad (28.66° N, 77.45° E) has experienced extensive deforestation due to the construction and highway projects and was declared the second most polluted city by the world air quality report of 2018 (*2018* World Air Quality Report, 2018). Faridabad (28.40° N, 77.31° E), the fourth most polluted city in 2018 (*2018* World Air Quality Report, 2018), is the most populous city of Haryana and also is a leading industrial centre. Gautam Buddha Nagar (28.33° N, 77.60° E) is also equally polluted (*2018* World Air Quality Report, 2018; Dahiya et al., 2017). Despite having such enormous urbanization and high air pollution level, aerosol characteristics in the area are still less explored to the best of our knowledge.

2.2. Satellite aerosol products

In the present study, we analyzed MODIS Terra (MOD04C6.1) (with 10:30 equatorial overpass time) and MODIS Aqua (MYD04C6.1) (with 13:30 equatorial overpass time) C6.1 AOD observation (AOD_{MODIS}) and ground-based AERONET data ($AOD_{AERONET}$) from January 2010 to December 2019. MODIS level-2 AOD products over land are retrieved by two algorithms: Deep Blue (DB) and Dark Target (DT). These AOD products are updated over time to reduce uncertainty and enhance AOD retrieval quality based on improved cloud mask, better surface reflectance estimation, and aerosol model schemes. Thus, C6.1, the most recent version of the product, was released in 2017 (Gupta et al., 2016;

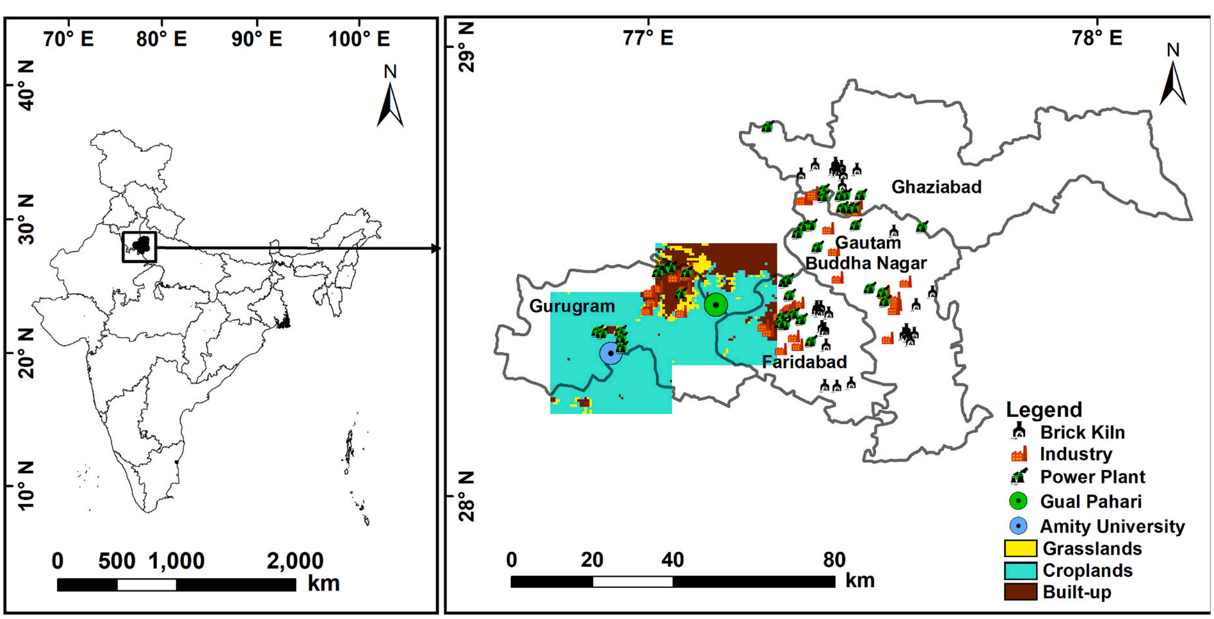

Fig. 1. Location of the study area and AERONET sites. LU/LC is extracted based on MCD12Q1 product of MODIS Land Cover at 500m resolution.

Levy et al, 2007, 2013bib_Levy_et_al_2013bib_Levy_et_al_2007; Remer et al., 2013). DB algorithm retrieves AOD at 10-km (DB_{10K}) resolution. DB algorithm was developed to retrieve aerosol properties over bright desert surfaces using deep-blue wavelength (0.47, or 0.412, 0.65 μm). In this algorithm, retrieval is performed at a 1-km resolution for the clear-sky pixels and then aggregated into a 10-km resolution (Hsu et al., 2006). Surface reflectance is assigned to the clear-sky pixels depending upon location, season, and the land cover type, from the look-up table (LUT) in visible bands (0.412, 0.47, 0.65 μm) at 10-km resolution. This algorithm's expected error envelope is ± (0.03 + 20% $AOD_{AERONET}$) (Bilal et al., 2018).

DT algorithm retrieves AOD at 10 km (DT_{10K}) and 3 km (DT_{3K}) resolution. Dark Target provides a better insight over the densely vegetated area. In a retrieval box of 10-km × 10-km, a group of 20 × 20 pixels with a resolution of 500 m at 0.47, 0.65, and 2.13 μm channels are organized. All the pixels with a reflectance of cloud, desert, snow/ice, and inland water and the remaining 20% darkest and 50% brightest pixels are discarded. Parametrization of two visible channel surface reflectance is done by a dynamic relationship between visible (0.47, 0.68 μm) and IR (2.13 μm) channels. According to geolocation and season, the aerosol model and LUT are employed for DT retrievals. After the matchup of radiance values in the LUT, spectral AOD can be obtained. Unlike DT_{10K}, the retrieval box is 3-km × 3-km and 36 pixels are organized for DT_{3K}. The expected error envelope for the 3-km product is ± (0.05 + 20% $AOD_{AERONET}$) (Levy et al., 2013), whereas, for the 10-km product, it is ± (0.05 + 15% $AOD_{AERONET}$) (Remer et al., 2005). The DT_{3K}, $DT_{10K,}$ and DB_{10K} AOD products are downloaded from https://ladsweb.modaps.eosdis.nasa.gov/for the present study. C6.1 DT AOD product has provided better insight for urban areas (urban area coverage > 20%) by using visible and SWIR band relationships for surface characterization in different parts of the world (Gupta et al., 2016).

2.3. AERONET aerosol product

Satellite aerosol products are validated using coincident AERONET-retrieved AOD data. The AERONET provides AOD data in 8 spectral bands with a high temporal resolution of 15 min by measuring spectral solar irradiance and sky radiance (Holben et al., 1998). $AOD_{AERONET}$ level 2.0 cloud screened and quality assured data has been processed for two sites - Gual Pahari and Amity University (locations shown in Fig. 1) in the study area from 2010 to 2019.

$AOD_{AERONET}$ is not available at 550 nm; therefore, the measurements are interpolated to 550 nm using Angstrom Exponent. Angstrom Exponent (α) is provided along with $AOD_{AERONET}$ and defined as:

$$\boldsymbol{\alpha} = -\frac{\ln\left(\frac{\tau 1}{\tau 2}\right)}{\ln\left(\frac{\lambda_1}{\lambda_2}\right)} \tag{1}$$

Here, τ_1 and τ_2 are the measurements of AOD at wavelengths λ_1 and $\lambda_{2,}$ respectively. The wavelengths used for the angstrom exponent are 675 nm and 440 nm.

Apart from aerosol data, MCD12Q1 land cover product with 500 m resolution has been used to obtain the diverse urban and rural land cover of the present study area. Details of all the data used in the present study have been provided in Table 1.

2.4. Methodology

The current methodology can be divided into i) Processing of AOD_{MODIS}, ii) Processing of $AOD_{AERONET}$ & iii) Validation of AOD_{MODIS} against $AOD_{AERONET}$. After evaluating the products, we have assessed the spatial and seasonal variations of AOD and examined the trends. All three - DT_{3K}, $DT_{10K,}$ and DB_{10K} AOD retrievals have been validated against the two AERONET sites in the current study. For DB_{10K}, the parameter "Deep_Blue_Aerosol_Optical_Depth_550_Land_Best_Estimate" with the highest quality assurance flag (QAF≥2) in the AOD product was analyzed. Likewise, we only processed the parameter "Optical_Depth_Land_And_Ocean" with the highest quality assurance flag (QAF = 3) for DT_{3K} and DT_{10K} AOD products.

AOD_{MODIS} is available at a wavelength of 550 nm, whereas the nearest available wavelength for $AOD_{AERONET}$ is 500 nm. Therefore, for a proper comparison and validation of AOD_{MODIS}, $AOD_{AERONET}$ at 500 nm is converted to $AOD_{AERONET}$ at 550 nm using equation (2) (Cesnulyte et al., 2014):

$$\boldsymbol{AOD}_{550nm} = \boldsymbol{AOD}_{500nm} \times \left(\frac{550}{500}\right)^{-\boldsymbol{\alpha}} \tag{2}$$

where α = angstrom exponent in 440–675 nm wavelength range (Sayer et al., 2013). Moreover, $AOD_{AERONET}$ measurement took place for a point at an average interval of 15 min. However, AOD_{MODIS} is a measurement of average aerosol for a particular area around the AERONET site twice a day. It is inappropriate to directly match the pixel value of AOD_{MODIS} with point-based AERONET measurements. Therefore, for the matchups, AOD_{MODIS} is spatially averaged in a 30 km × 30 km square box by taking AERONET locations as a central pixel to cover the heterogeneous landmasses and aerosol types (Xie et al., 2011). The AERONET instrument needs at least 1-h time to collect similar air mass monitored by the satellite data for accurate aerosol information in the dynamic

Table 1
Details of satellite and AERONET station data used.

Data	Scientific Data Sets (SDS)	Description	Resolution	Location	Time Period	Source
AERONET	Aerosol Optical Depth (V2)	Version 2 Direct Sun Algorithm	500 nm	Amity University	2010, 2016, 2017, 2018	http://aeronet.gsfc.nasa.gov/
				Gual Pahari	2017, 2018, 2019	
MOD04_L2, MOD04_3K	Optical_Depth_Land_And_Ocean	DT AOD at 550 nm over land and ocean	3 km,10 km (QAF = 3)	Gurugram, Faridabad, Ghaziabad, Gautam Buddha Nagar	2010–2019 2010–2019	https://ladsweb.modaps.eosdis.nasa.gov/
	Deep_Blue_Aerosol_Optical_Depth_550_Land_Best_Estimates	DB AOD at 550 nm over land	10 km (QAF = 2)			
MYD04_L2, MYD04_3K	Optical_Depth_Land_And_Ocean	DT AOD at 550 nm over land and ocean	3 km,10 km (QAF = 3)			
	Deep_Blue_Aerosol_Optical_Depth_550_Land_Best_Estimates	DB AOD at 550 nm over land	10 km (QAF = 2)			
MCD12Q1	International Geosphere-Biosphere Programme (IGBP) Classification	Land Cover Product	500m	Around AERONET Sites	2019	https://ladsweb.modaps.eosdis.nasa.gov/

atmosphere. $AOD_{AERONET}$ is provided in UTC (Coordinated Universal Time). Therefore, according to Indian standard time, the UTC has been converted to local time by adding 5.5 h to UTC for regional analysis. Temporal averaging of $AOD_{AERONET}$ at the AERONET site has been performed around Terra's overpass time window (10:00 am-12:00 pm) and Aqua (12:00 pm-2:00 pm) satellite. (Habib et al., 2019; Jiang et al., 2007; Zhang et al., 2016).

Due to the scarcity of the AERONET sites and limited ground measurements, statistical validation of AOD_{MODIS} has been possible for 2010, 2016, 2017, 2018, and 2019. Statistical analysis and matchups of AOD_{MODIS} with $AOD_{AERONET}$ has been performed using the concept of expected error by calculating Matchups (N), Correlation coefficient (R), Mean Absolute Error (MAE), Mean Bias (MB), Root Mean Square Error (RMSE), and Expected Error (EE) (Bilal et al., 2018; Levy et al., 2013; Mhawish et al., 2017; Remer et al, 2005, 2013bib_Remer_et_al_2013bib_Remer_et_al_2005). Details of equations used have been provided as Eq. no. 3–8.

$$MAE = \frac{1}{N}\sum_{i=1}^{N}\left|AOD_{(MODIS)i} - AOD_{(AERONET)i}\right| \tag{3}$$

$$MB = 1\Big/N\sum_{i=1}^{N}\left(AOD_{(MODIS)i} - AOD_{(AERONET)i}\right) \tag{4}$$

$$RMSE = \sqrt{\frac{1}{N}\sum_{i=1}^{N}\left(AOD_{(MODIS)i} - AOD_{(AERONET)i}\right)^2} \tag{5}$$

$$EE_{DB_{10K}} = \pm(0.03 + 0.20AOD_{AERONET}) \tag{6}$$

$$EE_{DT_{3K}} = \pm(0.05 + 0.20AOD_{AERONET}) \tag{7}$$

$$EE_{DT_{10K}} = \pm(0.05 + 0.15AOD_{AERONET}) \tag{8}$$

The matchups are categorized into three different types: i) above EE indicating overestimation; ii) within EE representing correct estimation, and iii) below EE exhibiting underestimation. According to previously published research, 66% of MODIS retrieved AOD falling within the EE envelope confirms the product's accuracy (Levy et al., 2013; Remer et al., 2005).

After the validation, we averaged daily DT_{10K} AOD to estimate the 10-year (2010–2019) mean values and assess the spatial and temporal variations over the study region. A 30 × 30 km buffer has been used considering AERONET sites as a central pixel to extract mixed land cover of the present study area from MCD12Q1 to get the variation of C6.1 derived AOD over different land cover types. The median values have been used to minimize the impact of outliers on the trend. The linear trend has been calculated by determining the slope for each grid point obtained from the linear fit. The statistically significant linear trends are determined using Student's t-test at a 95% significant level. Statistically considerable regions have been stippled for each season. Fig. 5, Fig. 6. The confidence levels of the trends have been calculated using Student's t-test:

$$t = r_{xy}\sqrt{\frac{N-2}{1-r_{xy}^2}} \tag{9}$$

where r_{xy} = correlation coefficient between the original time series and linear time series.

n = matchups.

3. Results

3.1. Validation of Aqua and Terra AOD (DB_{10K}, DT_{3K}, DT_{10K}) products

Considering the individual evaluation of DB and DT AOD products of Terra and Aqua satellite for each AERONET station, it can be remarked that DT has performed satisfactorily for the current study area with a larger number of matchups than DB and have a higher correlation with the ground measurement. The highest correlation between satellite and ground-based data at Amity University is found for the DT_{3K} product, with R ≈ 0.72 (AERONET-Terra) and 0.70 (AERONET-Aqua). At Gual Pahari station, the highest correlation is found for the DT_{10K} product with R ≈ 0.70 and 0.85, when comparing AERONET with Terra and Aqua, respectively. 63% (DT_{10K}) and 74% (DT_{3K}) of the total Terra AOD_{MODIS} retrievals and 58% (DT_{10K}) and 100% (DT_{10K}) of the total Aqua AOD_{MODIS} retrievals exist within the EE envelope at Amity University and Gual Pahari, respectively. For Amity University, Terra $DT_{10K,}$ and for Gual Pahari, Aqua DT_{10K} exhibits the highest number of AOD_{MODIS} retrievals within EE envelope (Table 2) indicating the very satisfactory performance of the aforementioned MODIS algorithms. For semi urbanized areas, the DT algorithm has a good performance along with the rural site of Amity University, where agricultural land is predominant. It is evident from the calculated MB, overall, both DB and DT algorithms underestimated AOD in the present study area for the examined period (2010–2019). Such observation contradicts the earlier findings that DT overestimated and DB underestimated AOD in the current study area from 2006 to 2015 (Mhawish et al., 2017). Compared to DT, the prominent underestimation of DB_{10K} AOD is evident from significant negative bias.

Considering the validation of AOD_{MODIS} using collective $AOD_{AERONET}$ from both the AERONET stations (Fig. 1), it has been observed that the correlation coefficient is higher for Aqua, with higher percentages of data samples falling within the EE envelope. Although the total number of matchups for the Aqua satellite is lesser than Terra (Table 3). Such results have confirmed the applicability of Aqua AOD_{MODIS} compared to Terra AOD_{MODIS} on the regional scale, which was reported earlier in the previously published research (Bright, and Gueymard, 2019); Tong et al., 2020; Wei et al., 2019). For both Terra and Aqua, DT_{10K} has retrieved AODs primarily within the EE compared to DB_{10K} and thus DT_{10K} has been accepted as a reliable algorithm for the current sites over other algorithms (Table 3). Comparing DT_{10K} AOD products of Terra and Aqua, it has been observed that Terra DT_{10K} slightly underestimated AOD while there is an equal proportion (12.9%) of Aqua DT_{10K} AOD lying above and below the EE envelope (Table 3). Such estimation error occurred due to the surface reflectance values and aerosol model assumption error for the current version of data C6.1 (Li et al., 2007; Xie et al., 2011). Moreover, such estimation error could be attributed to the less availability of $AOD_{AERONET}$ for validation.

Considering the upper and lower range of AOD, AOD_{MODIS} has been validated against $AOD_{AERONET}$ for three bins (i) AOD≤0.5, (ii) 0.5<AOD≤ 1, and (iii) AOD>1. A linear relationship has been observed between AOD_{MODIS} and $AOD_{AERONET}$ (Fig. 2). Observations are obtained mostly in the 0.5–1.0 AOD bin. Aqua AOD_{MODIS} is strongly correlated with $AOD_{AERONET}$ (R = 0.79). In the correlation analysis between AOD_{MODIS} and $AOD_{AERONET}$ (Fig. 2, Table 3), the slope is linked with systematic uncertainties, e.g., assumptions in the aerosol model and intercept show a deviation in surface reflectance estimation (Choudhry et al., 2012; Sayer et al., 2013). For the DT retrieved AOD, the high slope and intercept have specified infelicity in the aerosol type assumption and thereby estimated surface reflectance caused an error in retrieving AOD (Choudhry et al., 2012). In the 0.5–1.0 bin, more than 70% of AOD retrievals by Terra DT are falling within EE. On the other hand, less than 66% of AOD observations by Terra DB are falling within EE. Finally, it has been observed that DT performs better than DB_{10K} and DT AOD_{MODIS} between 0.5 and 1.0 are more correlated with the $AOD_{AERONET}$ than the rest (Table 4).

3.2. Spatial and seasonal variation of AOD

Seasonal variation of AOD could be attributed to the diverse meteorological conditions, aerosol sources, vegetation coverage, and crop

Table 2
Statistical summary of validation for DB_{10K}, DT_{3K} and DT_{10K} Terra and Aqua AOD_{MODIS} C6.1 using $AOD_{AERONET}$ of Amity University and Gual Pahari, Gurugram (N: Matchups, MB: Mean Bias, PWE: Percent Within Expected Error, PAE: Percent Above Expected Error, PBE: Percent Below Expected Error, MAE: Mean Absolute Error, R: Correlation coefficient).

			N	MB	PWE	PAE	PBE	MAE	R	Equation of Linear Regression
Amity University	**Terra**	**DB_{10K}**	40	−0.026	57.5	12.5	30	0.15	0.61	Y = 1.29*X-0.19
		DT_{3K}	59	−0.045	57.62	13.56	28.81	0.14	0.72	Y = 1.42*X-0.28
		DT_{10K}	49	−0.025	63.27	12.24	24.49	0.11	0.68	Y = 1.19*X-0.13
	Aqua	**DB_{10K}**	20	−0.121	55	5	40	0.15	0.67	Y = 0.86*X-0.04
		DT_{3K}	39	−0.00018	53.85	23.08	23.08	0.16	0.70	Y = 1.36*X-0.22
		DT_{10K}	38	0.022	57.89	21.05	21.05	0.16	0.68	Y = 1.52*X-0.29
Gual Pahari	**Terra**	**DB_{10K}**	29	−0.24	41.38	24.14	34.48	0.26	0.34	Y = 1.03*X-0.26
		DT_{3K}	31	−0.08	74.19	9.68	16.13	0.18	0.67	Y = 1.48*X-0.45
		DT_{10K}	33	−0.0317	54.55	18.18	27.27	0.18	0.70	Y = 1.36*X-0.33
	Aqua	**DB_{10K}**	18	−0.23	38.89	0.00	61.11	0.23	0.69	Y = 0.81*X-0.09
		DT_{3K}	26	−0.03	76.92	3.85	19.23	0.15	0.85	Y = 1.30*X-0.27
		DT_{10K}	24	−0.08	100	0	0	0.17	0.80	Y = 1.38*X-0.39

Table 3
Statistical summary of validation for DB_{10K}, DT_{3K} and DT_{10K} Terra and Aqua AOD_{MODIS} using collective $AOD_{AERONET}$ from both the AERONET stations (Amity University + Gual Pahari, Gurugram) (N: Matchups, PWE: Percent Within Expected Error, PAE: Percent Above Expected Error, PBE: Percent Below Expected Error, R: Correlation coefficient, RMSE: Root Mean Square Error).

	Terra AOD			Aqua AOD		
	DB_{10K}	DT_{3K}	DT_{10K}	DB_{10K}	DT_{3K}	DT_{10K}
N	69	90	82	38	65	62
PWE	50.72	52.22	53.66	47.37	63.08	74.19
PAE	17.39	6.67	12.20	2.63	15.38	12.90
PBE	31.88	17.78	18.29	50.00	21.54	12.90
R	0.44	0.74	0.77	0.70	0.79	0.72
RMSE	0.26	0.01	0.17	0.24	0.20	0.24
EQUATION OF LINEAR REGRESSION	Y = 1.06*X-0.15	Y = 1.30*X-0.24	Y = 1.20*X-0.15	Y = 0.78*X-0.03	Y = 1.06*X-0.15	Y = 1.35*X-0.25

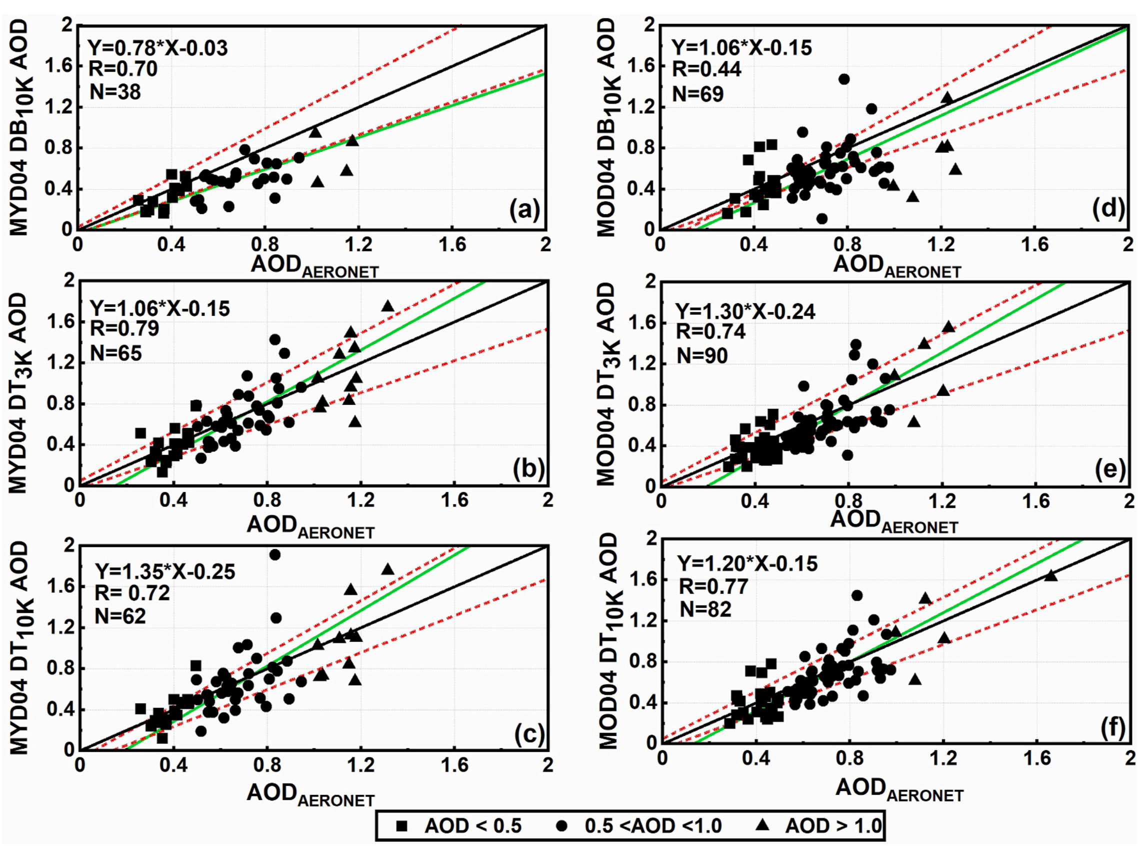

Fig. 2. Validation of AOD_{MODIS} against $AOD_{AERONET}$ over Amity University and Gual Pahari, Gurugram. MODIS AQUA (MYD04C6.1) (a, b, c) and MODIS TERRA (MOD04C6.1) (d, e, f). The green line represents a regression line, the dashed red lines shows expected error, and the solid black line is 1:1 line.

Table 4
Statistical summary of validation for DB_{10K}, DT_{3K} and DT_{10K} Terra and Aqua AOD_{MODIS} using collective $AOD_{AERONET}$ from both the AERONET stations (Amity University + Gual Pahari, Gurugram) in each bin (N: Matchups, PWE: Percent Within Expected Error, PAE: Percent Above Expected Error, PBE: Percent Below Expected Error).

		Terra AOD			Aqua AOD		
		<0.5	**0.5–1.0**	**>1**	**<0.5**	**0.5–1.0**	**>1**
N		29	37	3	20	18	0
DB_{10K}	**PWE**	44.82	56.75	33.33	35	50	0
	PAE	3.44	24.32	66.66	0	5.55	0
	PBE	51.72	18.91	0	65	44.44	0
N		40	42	8	21	34	10
DT_{3K}	**PWE**	57.5	73.80	37.5	57.14	70.58	50
	PAE	2.5	11.90	62.5	0	11.76	50
	PBE	40	14.28	0	42.85	14.70	0
N		30	44	8	21	31	10
DT_{10K}	**PWE**	46.66	70.45	25	71.42	80.64	60
	PAE	6.66	13.63	37.5	4.76	9.67	40
	PBE	46.66	15.90	0	23.80	9.67	0

growth phases, dominant in the present study area (Dey et al., 2020; Dey and Di Girolamo, 2010; Mangla et al., 2020; Mhawish et al., 2017). Subsequently, varied surface reflectance affects the retrieval of aerosol optical properties. Through seasonal distribution, it has been observed that AOD is high in the monsoon and the pre-monsoon season as well. Being in the semi-arid climatic zone, the present study area is affected by dust storms during the pre-monsoon season, which could be one of the prominent factors leading to high AOD during this season (Bilal et al., 2017; Dey et al., 2004; Mangla et al., 2020; Mhawish et al., 2017). Although, the notion is that cloud and precipitation may remove aerosols via washout and rainout, still, aerosol-precipitation linkage could not be conclusively established over Indian scenario because of the erratic rainfall (Kharol et al., 2013). Due to the light rain, aerosols particles become more concentrated because of increased humidity in the air. Large emission strength (from large to small scale industries, thermal power plants, brick kilns, vehicular emission, construction dust, road dust, household emissions, diesel generators, etc.) causes a rapid build-up of aerosol loading after a precipitation event (Chowdhury et al., 2016). Most importantly, AOD retrieval during the monsoon is biased towards dry days (Dey and Di Girolamo, 2010) as the passive sensor cannot retrieve AOD in presence of clouds. Therefore, the relatively clean condition is not captured in the climatology. Multiyear 2010–2019 average has depicted that both Terra DT_{10K} and Aqua DT_{10K} retrieved high AOD during monsoon and pre-monsoon season. While during the post-monsoon and winter season, low AOD has been observed (Fig. 4).

In Fig. 3, seasonal AOD_{MODIS} has been matched against $AOD_{AERONET}$. A much greater number of matchups have been observed for pre-monsoon and monsoon compared to winter and post-monsoon (Fig. 3). Unfortunately, during post-monsoon and winter, because of the deficit of AERONET observations, there are not enough statistics to remark about the AOD variation in those seasons. Contrary to the previous studies carried over the IGP region, where during monsoon retrieved AODs are mostly outside the error envelope (Tripathi et al., 2005), in the present study, more than 60% of retrieved AOD by DB_{10K}, $DT_{10K,}$ and DT_{3K} are within the EE envelope for the monsoon season. More than 20% of retrieved AOD by DB_{10K} (28%) are below the EE envelope. Unlike DB, for DT_{3K} and DT_{10K}, 21% and 22% of retrieved AOD are above the expected error envelope, respectively. During pre-monsoon, 43%–63% of AOD_{MODIS} observations have been retrieved within expected error for DB_{10K} (43.18%), DT_{10K} (54.34%), and DT_{3K} (62.26%) respectively. AOD_{MODIS} retrieved by DT_{3K} is highly correlated with $AOD_{AERONET}$ for monsoon (0.78) as well as for pre-monsoon (0.85). Overall, DT_{3K} has a good performance for pre-monsoon and monsoon seasons with the highest percentage of observations within EE and high R-value (Table 5).

However, detailed seasonal-wise validation of AOD_{MODIS} and thereby conclusive judgment about the performance of the product cannot be confirmed with full confidence as limited AERONET observations are available for the present study area. Availability of AERONET observations at regular intervals could improve the accuracy of the season-wise correlation analysis between AOD_{MODIS} and $AOD_{AERONET}$. Although, a genuine effort has been put forth to generate information in this data-scarce region which could highlight the need for implementation of a good network of AERONET stations and thereby systematic monitoring of AOD.

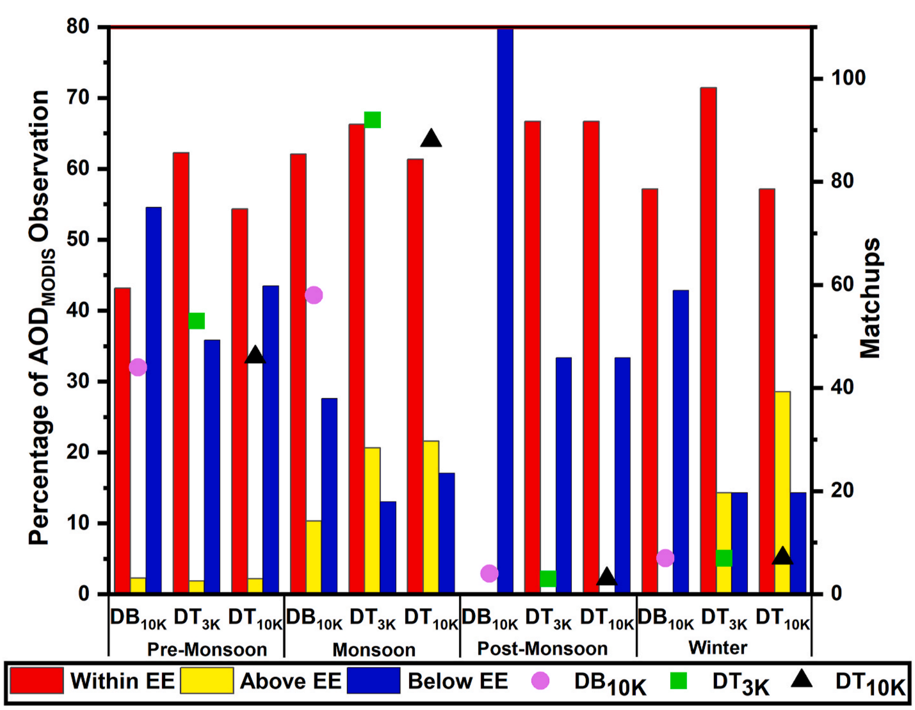

Fig. 3. Inter-seasonal variation and comparison of $AOD_{AERONET}$ and AOD_{MODIS}.

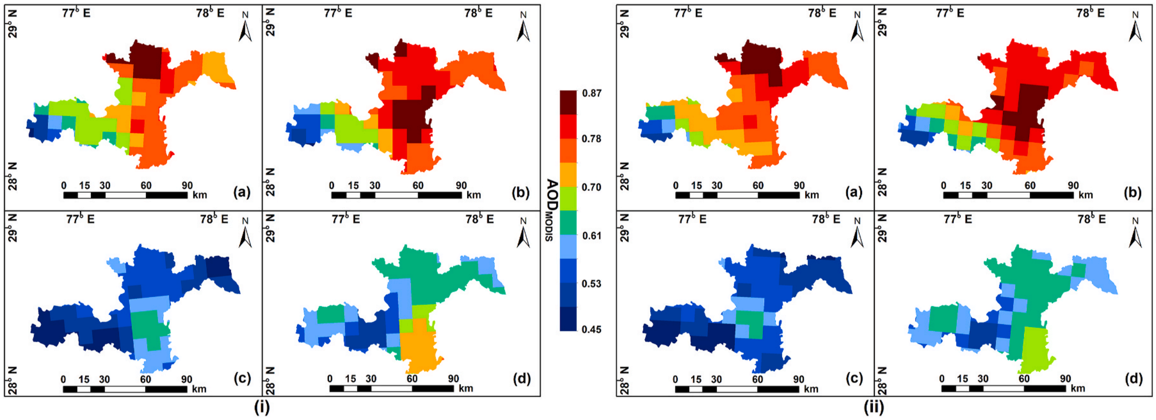

Fig. 4. Seasonal distribution of 10 years (2010–2019) average AOD_{MODIS} (i) MODIS AQUA (MYD04C6.1) DT_{10K} and (ii) MODIS TERRA (MOD04C6.1) DT_{10K} (a) Pre-Monsoon (b)Monsoon, (c) Post-Monsoon and (d) Winter.

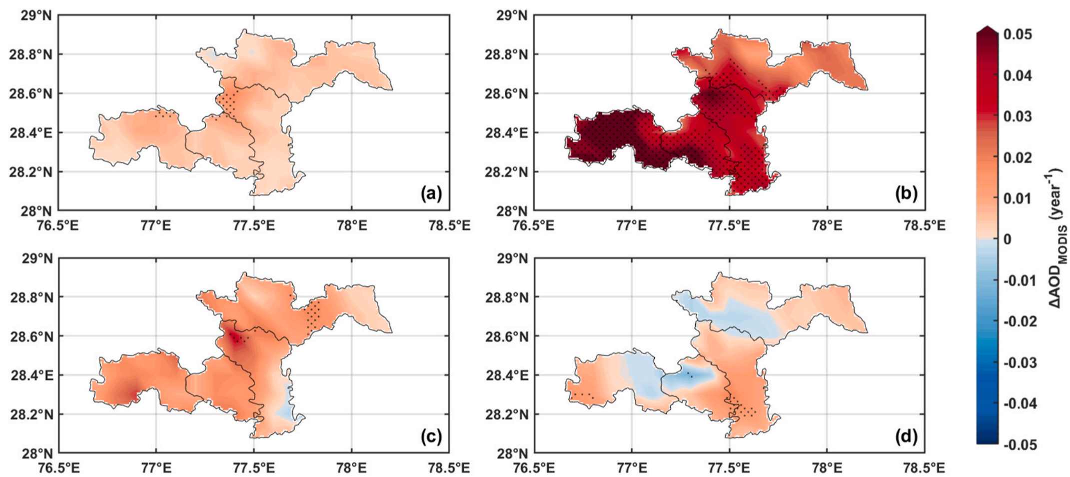

Fig. 5. Statistical significance and trend for AOD from MODIS AQUA (MYD04C6.1) DT_{10K} during the (a) Pre-Monsoon (b) Monsoon, (c) Post-Monsoon and (d) Winter during the period 2010–2019.

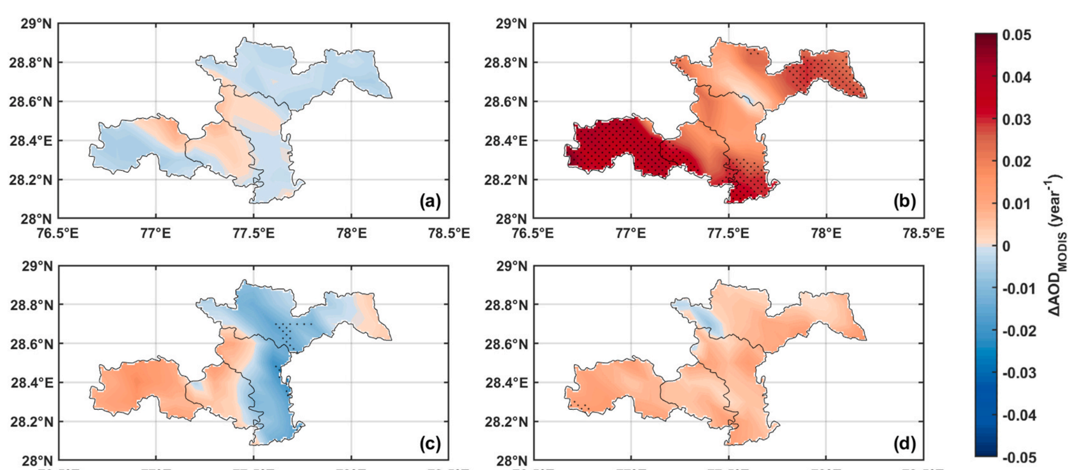

Fig. 6. Statistical significance and trend for AOD from MODIS TERRA (MOD04C6.1) DT_{10K} during the (a) Pre-Monsoon (b) Monsoon, (c) Post-Monsoon and (d) Winter during the period 2010–2019.

3.3. Trend analysis

To recognize the inter-annual variation of AOD, the annual trend has been analyzed for MODIS Aqua and MODIS Terra DT_{10K} AOD products during different seasons as DT_{10K} has performed well for the present study area compared to other algorithms. Furthermore, the Student's T-test has been used to calculate the statistical significance of the observed trend (Dey and Di Girolamo, 2011). The observed AOD trends are

Table 5
Statistical summary of validation for DB_{10K}, DT_{3K} and DT_{10K} AOD_{MODIS} (Terra + Aqua) using collective $AOD_{AERONET}$ from both the AERONET stations (Amity University + Gual Pahari, Gurugram) for each season (N: Matchups, MB: Mean Bias, PWE: Percent Within Expected Error, PAE: Percent Above Expected Error, PBE: Percent Below Expected Error, MAE: Mean Absolute Error, R: Correlation coefficient).

Algorithm	Season	N	MB	PWE	PAE	PBE	MAE	R
DB_{10K}	Pre-Monsoon	44	−0.19	43.18	2.27	54.54	0.22	0.72
	Monsoon	58	−0.08	62.06	10.34	27.58	0.18	0.40
	Post-Monsoon	4	−0.13	0	0	100	0.13	0.06
	Winter	7	−0.15	57.14	0	42.85	0.01	0.88
DT_{3K}	Pre-Monsoon	53	−0.12	62.26	1.88	35.84	0.16	0.85
	Monsoon	92	0.01	66.3	20.65	13.04	0.15	0.78
	Post-Monsoon	3	−0.11	66.66	0	33.33	0.11	−0.23
	Winter	7	0.01	71.42	14.28	14.28	0.02	0.92
DT_{10K}	Pre-Monsoon	46	−0.13	54.34	2.17	43.47	0.14	0.73
	Monsoon	88	0.03	61.36	21.59	17.04	0.15	0.77
	Post-Monsoon	3	−0.09	66.66	0	33.33	0.09	0.64
	Winter	7	0.02	57.14	28.57	14.28	0.02	0.92

considered statistically significant at the 95% confidence level when the p-value is < 0.05 according to Student's T-test. It should be mentioned that the trends for Aqua and Terra DT_{10K} retrieved AOD have been analyzed individually because of the overpass time difference of the two satellites causing an imbalance in AOD pattern during morning and afternoon timings. Therefore, the observations from Terra and Aqua could not be alike and comparable (Bright, and Gueymard, 2019)(.

In the current study, compared to other seasons, Aqua AOD has exhibited a stronger increasing trend during monsoon (Figs. 5 and 6). Unlike monsoon, comparatively weaker increasing trends have been observed during other seasons. The regionally averaged linear trend in MODIS Aqua AOD, is 0.0050 $year^{-1}$, 0.0352 $year^{-1}$ & 0.0131 $year^{-1}$, 0.0043 $year^{-1}$, for pre-monsoon, monsoon, and post-monsoon, winter, respectively. For Terra AOD, a significant increasing trend has been observed for monsoon whereas a relatively weaker decreasing trend has been observed during pre-monsoon and post-monsoon. The regionally averaged linear trend in MODIS Terra AOD, trend is, −0.0010 $year^{-1}$, 0.0235 $year^{-1}$ & −0.0011 $year^{-1}$, 0.0064 $year^{-1}$ for pre-monsoon, monsoon, and post-monsoon, winter, respectively. Although, it has been established from the validation results that Aqua AOD_{MODIS} has performed better compared to Terra in the present study area. Even the previously published research has also highlighted the superiority of MODIS Aqua AOD over Terra in explaining the annual AOD trend, especially in the land areas. MODIS Aqua AOD has taken that lead because of the different overpass time of Terra, Aqua. Therefore, the two platforms have encountered the imbalance of AOD pattern during afternoon/morning. Moreover, rapid degradation of the Terra instrument has affected the quality of data (Bright, and Gueymard, 2019); Wei et al., 2019).

Increasing aerosol trend during monsoon observed in the present study has been reported in earlier studies also for Indian regions (Jin and Wang, 2018; Wei et al., 2019). Over the past decade, NCR has witnessed unexpected spatial growth with an urbanization level of 62.5% in 2011 expecting to touch 71% by 2021, multifarious increase in the vehicle, development of a total of 53 industrial hubs with large-medium-small scale industries, and 1509 brick kilns (Kumar and Nivit, 2018; National Capital Region Planning Board, 2015; Verma, 2017). Apart from the urban area, the rural area of north-western India adds substantially to aerosol loading especially during the monsoon (Kharif season-June to September) by intensive conventional cultivation and application of fertilizer (Campbell et al., 2017; Kuttippurath et al., 2020). Due to such dominant anthropogenic factors, even after the prominent increase of green cover and monsoonal rainfall in the Northwest Indian subcontinent since 2002, a declining AOD trend has been observed only in the dust source region rather than in entire north-western India (Jin and Wang, 2018). Hence, a detailed analysis of driving forces responsible for a substantial increase in AOD can be considered as the future scope of the study.

4. Discussion and conclusions

A vast country like India is not equipped with a robust network of ground-based measurements of columnar aerosol properties (that are freely disseminated for scientific applications), which has been considered as a limitation of aerosol studies. Such limitations could be complemented with satellite measurement. Here we evaluated the latest (C6.1) Terra, Aqua, DT_{3K}, DT_{10K}, and DB_{10K} aerosol products with ground-based AERONET measurements over 10 years (2010–2019) for the data-scarce region of Delhi, NCR.

Although underestimation of AOD has been observed for all the algorithms, a prominent underestimation of DB_{10K} AOD has been observed compared to DT. Updated collection 6.1 DT AOD products have worked well for both the sites of Amity University (rural site) and Gual Pahari (semi-urban site) by retrieving AOD within expected error and having a strong correlation with ground measurement. Aqua AOD shows a higher correlation within expected error than Terra AOD in this region. The possible reason for Aqua's best performance could be due to the flight timing difference between the two sensors and rapid degradation of the Terra instrument. Significant emission from different sources in the highly urbanized study area, overutilization of fertilizer in intensive conventional cultivation during Kharif season causes an abrupt escalation of aerosol loading after light rainfall. Despite the greening in the northwest region, unplanned urbanization and resultant anthropogenic activities have played a vital role to increase the aerosol concentration in the present study area. Although, the inability of the passive sensor to capture AOD in cloudy days could be considered as a limitation of AOD monitoring during monsoon.

Such a study would provide a base for air quality assessment in the highly urbanized cities to grab the attention of planners or policymakers working towards climate adaptation and mitigation for achieving sustainable development goals. The present study can further help to identify locations with a high aerosol load that needs continuous monitoring by installing AERONET stations. Such studies can benefit society by keeping them aware of long-term pollution levels in their surroundings. Although satellite remote sensing has played a dynamic role in compensating data scarcity, there is still a need to validate satellite observations with ground measurements. The scarcity of ground observation has been observed as the limitation, and the installation of AERONET stations at regular intervals can improve the work's accuracy. Therefore, the present study has recommended establishing a more significant number of AERONET sites and the systematic recording of the long-term AOD in the study area.

Credit author statement

Vipasha Sharma: Formal analysis, Investigation, Data Curation, Writing - Original Draft, Visualization Swagata Ghosh: Conceptualization, Investigation, Writing - Review & Editing, Supervision, Project administration, Funding acquisition Muhammad Bilal: Software, Formal analysis, Writing - Review & Editing Sagnik Dey: Software, Formal analysis, Writing - Review & Editing Sultan Singh: Resources. Supervision.

Declaration of competing interest

The authors declare that they have no known competing financial interests or personal relationships that could have appeared to influence the work reported in this paper.

Acknowledgements

The corresponding author acknowledges the Science & Engineering Research Board (SERB), Department of Science & Technology (DST), Government of India for funding this work through Project File No. ECR/2017/000331.

The authors would like to thank NASA for the MODIS aerosol product and Principle Investigators Dr. Panuganti C. S. Devara and Dr. Antti Arola of AEORNET stations for their endeavours in establishing, recording, and maintaining long-term aerosol data. Dr. Sagnik Dey acknowledges support from IIT Delhi for the Institute Chair position.

The authors thank the editor and anonymous reviewers for their valuable suggestions and comment which enriched the manuscript.

References

Alpert, P., Shvainshtein, O., Kishcha, P., 2012. AOD trends over megacities based on space monitoring using MODIS and MISR. Am. J. Clim. Change 117–131. https://doi.org/10.4236/ajcc.2012.13010, 01.

Bender, F.A.M., Frey, L., McCoy, D.T., Grosvenor, D.P., Mohrmann, J.K., 2019. Assessment of aerosol–cloud–radiation correlations in satellite observations, climate models and reanalysis. Clim. Dynam. 52, 4371–4392. https://doi.org/10.1007/s00382-018-4384-z.

Bilal, M., Nichol, J.E., Spak, S.N., 2017. A new approach for estimation of fine particulate concentrations using satellite aerosol optical depth and binning of meteorological variables. Aerosol Air Qual. Res. 17, 356–367. https://doi.org/10.4209/aaqr.2016.03.0097.

Bilal, M., Qiu, Z., Campbell, J.R., Spak, S.N., Shen, X., Nazeer, M., 2018. A new MODIS C6 dark target and Deep Blue merged aerosol product on a 3 km spatial grid. Rem. Sens. 10, 1–13. https://doi.org/10.3390/rs10030463.

Bilal, M., Nazeer, M., Nichol, J., Qiu, Z., Wang, L., Bleiweiss, M.P., Shen, X., Campbell, J. R., Lolli, S., 2019. Evaluation of terra-MODIS C6 and C6.1 aerosol products against Beijing, XiangHe, and Xinglong AERONET sites in China during 2004-2014. Rem. Sens. 11 https://doi.org/10.3390/rs11050486.

Boucher, O., Haywood, J., 2001. On summing the components of radiative forcing of climate change. Clim. Dynam. 18, 297–302. https://doi.org/10.1007/s003820100185.

Bright, J.M., Gueymard, C.A., 2019. Climate-specific and global validation of MODIS Aqua and Terra aerosol optical depth at 452 AERONET stations. Sol. Energy 183, 594–605. https://doi.org/10.1016/j.solener.2019.03.043.

Campanelli, M., Estellés, V., Diemoz, H., Kouremeti, N., Kazadzis, S., Becker, R., Vergari, S., Dietrich, S., 2015. The SKYNET Radiometer Network : Aerosol Optical Depth Retrieval Performance at the FRC-IV Campaign and Long-Term Comparison against GAW-PFR and AERONET Standard Instruments, vol. 29, pp. 3–29. P3.

Campbell, B.M., Beare, D.J., Bennett, E.M., Hall-Spencer, J.M., Ingram, J.S.I., Jaramillo, F., Ortiz, R., Ramankutty, N., Sayer, J.A., Shindell, D., 2017. Agriculture production as a major driver of the earth system exceeding planetary boundaries. Ecol. Soc. 22 https://doi.org/10.5751/ES-09595-220408.

Census of India, 2011. Cities Having Population 1 Lakh and above.

Cesnulyte, V., Lindfors, A.V., Pitkänen, M.R.A., Lehtinen, K.E.J., Morcrette, J.J., Arola, A., 2014. Comparing ECMWF AOD with AERONET observations at visible and UV wavelengths. Atmos. Chem. Phys. 14, 593–608. https://doi.org/10.5194/acp-14-593-2014.

Choudhry, P., Misra, A., Tripathi, S.N., 2012. Study of MODIS derived AOD at three different locations in the indo gangetic plain: kanpur, gandhi college and nainital. Ann. Geophys. 30, 1479–1493. https://doi.org/10.5194/angeo-30-1479-2012.

Chowdhury, S., Dey, S., Ghosh, S., Saud, T., 2016. Satellite-based estimates of aerosol washout and recovery over India during monsoon. Aerosol Air Qual. Res. 16, 1302–1314. https://doi.org/10.4209/aaqr.2015.01.0018.

Chowdhury, S., Dey, S., Di Girolamo, L., Smith, K.R., Pillarisetti, A., Lyapustin, A., 2019. Tracking Ambient PM 2.5 Build-Up in Delhi National Capital Region during the Dry Season over 15 Years Using a High-Resolution (1 Km) Satellite Aerosol Dataset. https://doi.org/10.1016/j.atmosenv.2019.02.029.

Christopher, S., Gupta, P., 2020. Global distribution of column satellite aerosol optical depth to surface PM2.5 relationships. Rem. Sens. 12, 1–13. https://doi.org/10.3390/rs12121985.

Colbeck, I., Lazaridis, M., 2010. Aerosols and environmental pollution. Naturwissenschaften 97, 117–131. https://doi.org/10.1007/s00114-009-0594-x.

Dahiya, S., Myllyvirta, L., Sivalingam, N., 2017. Airpocalyse- Assessment of Air Pollution in Indian Cities. https://doi.org/10.1080/19485565.1983.9988543.

Dey, S., Di Girolamo, L., 2010. A climatology of aerosol optical and microphysical properties over the Indian subcontinent from 9 years (2000-2008) of Multiangle Imaging Spectroradiometer (MISR) data. J. Geophys. Res. Atmos. 115, 1–22. https://doi.org/10.1029/2009JD013395.

Dey, S., Di Girolamo, L., 2011. A decade of change in aerosol properties over the Indian subcontinent. Geophys. Res. Lett. 38, 1–5. https://doi.org/10.1029/2011GL048153.

Dey, S., Tripathi, S.N., Singh, R.P., Holben, B.N., 2004. Influence of dust storms on the aerosol optical properties over the Indo-Gangetic basin. J. Geophys. Res. Atmos. 109, 1–13. https://doi.org/10.1029/2004JD004924.

Dey, S., Di Girolamo, L., van Donkelaar, A., Tripathi, S.N., Gupta, T., Mohan, M., 2012. Variability of outdoor fine particulate (PM 2.5) concentration in the Indian Subcontinent: a remote sensing approach. Remote Sens. Environ. 127, 153–161. https://doi.org/10.1016/j.rse.2012.08.021.

Dey, S., Purohit, B., Balyan, P., Dixit, K., Bali, K., 2020. A satellite – based high-resolution (1-km) ambient PM 2 . 5 database for India over two decades quality management. Int. J. Rem. Sens.

Gupta, P., Levy, R.C., Mattoo, S., Remer, L.A., Munchak, L.A., 2016. A surface reflectance scheme for retrieving aerosol optical depth over urban surfaces in MODIS Dark Target retrieval algorithm. Atmos. Meas. Tech. 9, 3293–3308. https://doi.org/10.5194/amt-9-3293-2016.

Habib, A., Chen, B., Khalid, B., Tan, S., Che, H., Mahmood, T., Shi, G., Butt, M.T., 2019. Estimation and inter-comparison of dust aerosols based on MODIS, MISR and AERONET retrievals over Asian desert regions. J. Environ. Sci. (China) 76, 154–166. https://doi.org/10.1016/j.jes.2018.04.019.

Holben, B.N., Eck, T.F., Slutsker, I., Tanré, D., Buis, J.P., Setzer, A., Vermote, E., Reagan, J.A., Kaufman, Y.J., Nakajima, T., Lavenu, F., Jankowiak, I., Smirnov, A., 1998. Aeronet - a federated instrument network and data archive for aerosol characterization. Remote Sens. Environ. 66, 1–16. https://doi.org/10.1016/S0034-4257(98)00031-5.

Hsu, N.C., Tsay, S.C., King, M.D., Herman, J.R., 2006. Deep Blue retrievals of Asian aerosol properties during ACE-Asia. IEEE Trans. Geosci. Rem. Sens. 44, 3180–3195. https://doi.org/10.1109/TGRS.2006.879540.

Huang, Y., Zhu, B., Zhou, X., Chen, D., Zhu, Z., Zhang, T., Gong, W., Ji, Y., Xia, X., Wang, L., 2019. Evaluation and comparison of MODIS collection 6.1 and collection 6 dark target aerosol optical depth over mainland China under various conditions including spatiotemporal distribution, haze effects, and underlying surface. Earth Sp. Sci. 6, 2575–2592. https://doi.org/10.1029/2019EA000809.

Jalan, I., 2019. What is Polluting Delhi ' s Air ? Understanding Uncertainties in Emissions Inventories.

Jiang, X., Liu, Y., Yu, B., Jiang, M., 2007. Comparison of MISR aerosol optical thickness with AERONET measurements in Beijing metropolitan area. Remote Sens. Environ. 107, 45–53. https://doi.org/10.1016/j.rse.2006.06.022.

Jin, Q., Wang, C., 2018. The greening of Northwest Indian subcontinent and reduction of dust abundance resulting from Indian summer monsoon revival. Sci. Rep. 8, 1–9. https://doi.org/10.1038/s41598-018-23055-5.

Kahn, R.A., 2012. Reducing the uncertainties in direct aerosol radiative forcing. Surv. Geophys. 33, 701–721. https://doi.org/10.1007/s10712-011-9153-z.

Kaufman, Y.J., Tanré, D., Boucher, O., 2002. A satellite view of aerosols in the climate system. Nature 419, 215–223. https://doi.org/10.1038/nature01091.

Kharol, S.K., Kaskaoutis, D.G., Sharma, A.R., Singh, R.P., 2013. Long-term (1951-2007) rainfall trends around six Indian cities: current state, meteorological, and urban dynamics. Adv. Meteorol. 2013. https://doi.org/10.1155/2013/572954.

Kompalli, S.K., Suresh Babu, S., Krishna Moorthy, K., 2010. Inter-comparison of aerosol optical depth from the Multi-Wavelength Solar Radiometer with other radiometric measurements. Indian J. Radio Space Phys. 39, 364–371.

Kumar, R., Nivit, Y.K., 2018. MAKEOVER: Conversion of Brick Kilns in Delhi-NCR to a Cleaner Technology—A Status Report. Centre for Science and Environment, New Delhi.

Kuttippurath, J., Singh, A., Dash, S.P., Mallick, N., Clerbaux, C., Van Damme, M., Clarisse, L., Coheur, P.F., Raj, S., Abbhishek, K., Varikoden, H., 2020. Record high levels of atmospheric ammonia over India: spatial and temporal analyses. Sci. Total Environ. 740, 139986. https://doi.org/10.1016/j.scitotenv.2020.139986.

Levy, R.C., Remer, L.A., Mattoo, S., Vermote, E.F., Kaufman, Y.J., 2007. Second-generation operational algorithm: retrieval of aerosol properties over land from inversion of Moderate Resolution Imaging Spectroradiometer spectral reflectance. J. Geophys. Res. Atmos. 112, 1–21. https://doi.org/10.1029/2006JD007811.

Levy, R.C., Mattoo, S., Munchak, L.A., Remer, L.A., Sayer, A.M., Patadia, F., Hsu, N.C., 2013. The Collection 6 MODIS aerosol products over land and ocean. Atmos. Meas. Tech. 6, 2989–3034. https://doi.org/10.5194/amt-6-2989-2013.

Li, Z., Niu, F., Lee, K.H., Xin, J., Hao, W.M., Nordgren, B., Wang, Y., Wang, P., 2007. Validation and understanding of Moderate Resolution Imaging Spectroradiometer aerosol products (C5) using ground-based measurements from the handheld Sun photometer network in China. J. Geophys. Res. Atmos. 112 https://doi.org/10.1029/2007JD008479.

Mangla, R., J, I., Chakra, S.S., 2020. Inter-comparison of multi-satellites and aeronet AOD over Indian region. Atmos. Res. 240, 104950. https://doi.org/10.1016/j.atmosres.2020.104950.

Mhawish, A., Banerjee, T., Broday, D.M., Misra, A., Tripathi, S.N., 2017. Evaluation of MODIS Collection 6 aerosol retrieval algorithms over Indo-Gangetic Plain: implications of aerosols types and mass loading. Remote Sens. Environ. 201, 297–313. https://doi.org/10.1016/j.rse.2017.09.016.

Mishchenko, M.I., Geogdzhayev, I.V., Cairns, B., Carlson, B.E., Chowdhary, J., Lacis, A. A., Liu, L., Rossow, W.B., Travis, L.D., 2007. Past, present, and future of global aerosol climatologies derived from satellite observations: a perspective. J. Quant. Spectrosc. Radiat. Transf. 106, 325–347. https://doi.org/10.1016/j.jqsrt.2007.01.007.
Moorthy, K.K., Nair, P.R., Murthy, B.V.K., 1989. Multiwavelength solar radiometer network and features of aerosol spectral optical depth at Trivandrum. Indian J. Radio Space Phys. 18, 194–201.
Mukherjee, T., Vinoj, V., 2020. Atmospheric aerosol optical depth and its variability over an urban location in Eastern India. Nat. Hazards 102, 591–605. https://doi.org/10.1007/s11069-019-03636-x.
National Capital Region Planning Board, 2015. Economic Profile of NCR 2015 Final Report.
Remer, L.A., Kaufman, Y.J., Tanré, D., Mattoo, S., Chu, D.A., Martins, J.V., Li, R.R., Ichoku, C., Levy, R.C., Kleidman, R.G., Eck, T.F., Vermote, E., Holben, B.N., 2005. The MODIS aerosol algorithm, products, and validation. J. Atmos. Sci. 62, 947–973. https://doi.org/10.1175/JAS3385.1.
Remer, L.A., Mattoo, S., Levy, R.C., Munchak, L.A., 2013. MODIS 3 km aerosol product: algorithm and global perspective. Atmos. Meas. Tech. 6, 1829–1844. https://doi.org/10.5194/amt-6-1829-2013.
Ren-Jian, Z., Kin-Fai, H., Zhen-Xing, S., 2012. The role of aerosol in climate change, the environment, and human health. Atmos. Oceanogr. Sci. Libr. 5, 156–161. https://doi.org/10.1080/16742834.2012.11446983.
Sai Suman, M.N., Gadhavi, H., Ravi Kiran, V., Jayaraman, A., Rao, S.V.B., 2014. Role of coarse and fine mode aerosols in MODIS AOD retrieval: a case study over southern India. Atmos. Meas. Tech. 7, 907–917. https://doi.org/10.5194/amt-7-907-2014.
Sano, I., Mukai, S., Yamano, M., Takamura, T., Nakajima, T., Holben, B., 2003. Calibration and validation of retrieved aerosol properties based on aeronet and skynet. Adv. Space Res. 32, 2159–2164. https://doi.org/10.1016/S0273-1177(03)90538-2.
Sayer, A.M., Hsu, N.C., Bettenhausen, C., Jeong, M.J., 2013. Validation and uncertainty estimates for MODIS Collection 6 "deep Blue" aerosol data. J. Geophys. Res. Atmos. 118, 7864–7872. https://doi.org/10.1002/jgrd.50600.
SDG Vision Haryana, 2030, 2017.
Srivastava, P., Dey, S., Agarwal, P., Basil, G., 2014. Aerosol characteristics over Delhi national capital region: a satellite view. Int. J. Rem. Sens. 35, 5036–5052. https://doi.org/10.1080/01431161.2014.934404.
Tian, X., Liu, Q., Li, X., Wei, J., 2018. Validation and comparison of MODIS C6.1 and C6 aerosol products over Beijing, China. Rem. Sens. https://doi.org/10.3390/rs10122021.
Tong, Y., Feng, L., Sun, K., Tang, J., 2020. Assessment of the representativeness of MODIS aerosol optical depth products at different temporal scales using global AERONET measurements. Rem. Sens. 12, 2330. https://doi.org/10.3390/rs12142330.
Tripathi, S.N., Dey, S., Chandel, A., Srivastava, S., Singh, R.P., Holben, B.N., 2005. Comparison of MODIS and AERONET derived aerosol optical depth over the Ganga Basin, India. Ann. Geophys. 23, 1093–1101. https://doi.org/10.5194/angeo-23-1093-2005.
Tuna Tuygun, G., Ozdemir, E., Elbir, T., 2020. Evaluation of MODIS C6 and C6.1 Dark Target AOD products over Turkey based on NDVI and aerosol type. Atmos. Pollut. Res. 1–15. https://doi.org/10.1016/j.apr.2020.07.003.
Verma, R.C., 'B ', S., 2017. Urbanisation in Delhi- NCR(National Capital Region). KPMG.
Wei, J., Peng, Y., Guo, J., Sun, L., 2019. Performance of MODIS Collection 6.1 Level 3 aerosol products in spatial-temporal variations over land. Atmos. Environ. 206, 30–44. https://doi.org/10.1016/j.atmosenv.2019.03.001.
WHO, 2016. Ambient Air Pollution: A Global Assessment of Exposure and Burden of Disease. World Health Organization.
Wild, M., Gilgen, H., Roesch, A., Ohmura, A., Long, C.N., Dutton, E.C., Forgan, B., Kallis, A., Russak, V., Tsvetkov, A., 2005. From dimming to brightening: decadal changes in solar radiation at earth's surface. Science 308, 847–850. https://doi.org/10.1126/science.1103215.
World Air Quality Report., 2018.
Xie, Y., Zhang, Y., Xiong, X., Qu, J.J., Che, H., 2011. Validation of MODIS aerosol optical depth product over China using CARSNET measurements. Atmos. Environ. 45, 5970–5978. https://doi.org/10.1016/j.atmosenv.2011.08.002.
Zhang, W., Gu, X., Xu, H., Yu, T., Zheng, F., 2016. Assessment of OMI near-UV aerosol optical depth over Central and East Asia. J. Geophys. Res. 121, 382–398. https://doi.org/10.1002/2015JD024103.